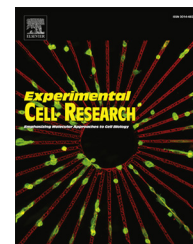


Available online at [www.sciencedirect.com](http://www.sciencedirect.com)

SciVerse ScienceDirect

journal homepage: [www.elsevier.com/locate/yexcr](http://www.elsevier.com/locate/yexcr)

## Research Article

# miR-138 overexpression is more powerful than hTERT knockdown to potentiate apigenin for apoptosis in neuroblastoma in vitro and in vivo

Mrinmay Chakrabarti<sup>a</sup>, Naren L. Banik<sup>b</sup>, Swapan K. Ray<sup>a,\*</sup><sup>a</sup>Department of Pathology, Microbiology, and Immunology, University of South Carolina School of Medicine, Columbia, SC, USA<sup>b</sup>Department of Neurosciences, Medical University of South Carolina, Charleston, SC, USA

## ARTICLE INFORMATION

## Article Chronology:

Received 7 January 2013

Received in revised form

21 February 2013

Accepted 22 February 2013

Available online 3 April 2013

## Keywords:

Apoptosis

Flow cytometry

hTERT shRNA

miR-138

Neuroblastoma

## ABSTRACT

Decrease in expression of the tumor suppressor microRNA-138 (miR-138) correlates well with an increase in telomerase activity in many human cancers. The ability of almost all human cancer cells to grow indefinitely is dependent on presence of telomerase activity. The catalytic component of human telomerase reverse transcriptase (hTERT) regulates telomerase activity in most of the human cancers including malignant neuroblastoma. We observed an indirect increase in the expression of miR-138 after the transfection with hTERT short hairpin RNA (shRNA) plasmid in human malignant neuroblastoma SK-N-DZ and SK-N-BE2 cell lines. Transfection with hTERT shRNA plasmid followed by treatment with the flavonoid apigenin (APG) further increased expression of miR-138. Direct transfection with miR-138 mimic was more powerful than transfection with hTERT shRNA plasmid in potentiating efficacy of APG for decreasing cell viability and colony formation capability of both cell lines. Upregulation of miR-138 was also more effective than down regulation of hTERT in enhancing efficacy of APG for induction of apoptosis in malignant neuroblastoma cells in vitro and in vivo. We delineated that apoptosis occurred with induction of molecular components of the extrinsic and intrinsic pathways in SK-N-DZ and SK-N-BE2 cells both in vitro and in vivo. In conclusion, these results demonstrate that direct miR-138 overexpression is more powerful than hTERT down regulation in enhancing pro-apoptotic effect of APG for controlling growth of human malignant neuroblastoma in cell culture and animal models.

© 2013 Elsevier Inc. All rights reserved.

## Introduction

Neuroblastoma is the most common extra cranial solid tumor in childhood. It usually arises in the adrenal gland but may also occur in abdominal, thoracic, cervical, or pelvic sympathetic ganglia [1]. These tumors are particularly noted for their extensive

heterogeneity in clinical behaviors, ranging from spontaneous regression to aggressive course. Malignant neuroblastomas in most cases show high rates of recurrence due to their poor response to the currently available therapeutic agents and many of these tumors ultimately cause death of the pediatric patients. In order to improve of the treatments for malignant neuroblastoma patients,

\*Corresponding author. Fax: +1 803 216 3428.

E-mail address: [swapan.ray@uscmed.sc.edu](mailto:swapan.ray@uscmed.sc.edu) (S.K. Ray).

new therapeutic approaches need to be explored based on the aberrant molecular features of these deadly tumors.

Aberrant expression of microRNAs (miRs) is often observed in different types of cancers [2]. Specific miRs function as tumor suppressors or oncogenes and thereby modulate many aspects of carcinogenesis [3]. These miRs may have diagnostic or prognostic values and are presumed to be potential therapeutic targets in the treatment of human malignant neuroblastomas. The alteration in expression of the tumor suppressor miR-138 has been frequently observed in a number of cancers including thyroid cancer, lung cancer, and leukemia [4–6]. Down regulation of miR-138 in head-and-neck squamous cell carcinoma is associated with mesenchymal-like cell morphology and enhanced cell migration and invasion [7]. It is important to note that miR-138 partially acts as a negative regulator of the human telomerase reverse transcriptase (hTERT), the catalytic subunit of telomerase, whereas multiple miRs potentially target the hTERT gene for its down regulation uniformly in human anaplastic thyroid carcinoma cell lines [4]. Increase in telomerase activity is associated with malignant growth of many tumors including neuroblastomas. Many recent studies have indicated that telomerase activity can be regulated by post-transcriptional mechanisms [8–14]. Therefore, post-transcriptional factors that are involved in the regulation of telomerase activity have generated considerable interest. Currently, miRs are considered to play a key role in modulating many post-transcriptional pathways. Considering the fact that an individual miR can target multiple oncogenic pathways, restoration of expression of a powerful tumor suppressor miR that is down regulated in cancer has attracted a lot of attention as a potential therapeutic option [15,16].

The introduction of a short hairpin RNA (shRNA) into the cells through a plasmid vector encoding specific shRNA and its expression is a very powerful technique to knockdown a particular mRNA molecule and subsequently the protein level of the targeted gene [17–19]. Down regulation of hTERT gene using hTERT shRNA plasmid vector can also be an effective way to inhibit telomerase activity, proliferation of cells, and thereby the growth of tumor. Current trends in cancer research show that flavonoids are highly favorite plant-derived compounds for using alone or in combination with another therapeutic agent for controlling the growth of various malignant cells both in vitro and in vivo. Apigenin (APG), a well known flavonoid present in fruits and vegetables, induces cell death by activation of both the extrinsic and intrinsic pathways of apoptosis in many cancers including human malignant neuroblastoma [20].

The aim of our present investigation was to make comparative studies to delineate the power of the miR-138 mimic and the hTERT shRNA plasmid in potentiating the efficacy of APG for modulating the molecular mechanisms for higher inhibition of cell proliferation and induction of apoptosis in human malignant neuroblastoma SK-N-DZ and SK-N-BE2 cells both in vitro and in vivo. Our study demonstrated that combination of miR-138 and APG was more potent than combination of hTERT shRNA and APG in sensitizing tumor cells to apoptosis. Therefore, combination therapeutic strategy using miR-138 mimic and APG can be a powerful therapeutic option for treatment of human malignant neuroblastomas. To the best of our knowledge, no study has yet been conducted for investigating the anti-tumor efficacy of the tumor suppressor miR-138 in human malignant neuroblastomas.

## Materials and methods

### Cell cultures and treatments

The human malignant neuroblastoma SK-N-DZ and SK-N-BE2 cell lines were procured from the American Type Culture Collection (ATCC, Manassas, VA, USA). Both SK-N-DZ and SK-N-BE2 cell lines were grown in DMEM medium supplemented with 10% fetal bovine serum (FBS) and 1% penicillin and 1% streptomycin (GIBCO/BRL, Grand Island, NY, USA). Cell lines were maintained in a fully-humidified incubator containing 5% CO<sub>2</sub> at 37 °C. The medium and FBS were purchased from Atlanta Biologicals (Norcross, GA, USA). APG, purchased from Sigma Chemical (St. Louis, MO, USA), was dissolved in dimethyl sulfoxide (DMSO) to make stocks and store at –20 °C. In all experiments, control cell cultures contained the same concentration of DMSO that was used in the treatment with APG. Concentration of DMSO in the experiments was maintained at less than 0.01%, which was not able to induce cell growth, differentiation, or death. hTERT shRNA plasmid was procured from Santa Cruz Biotechnology (Santa Cruz, CA, USA). miR-138 mimic was purchased from Dharmacon (Chicago, IL, USA).

### Transfection of SK-N-DZ and SK-N-BE2 cells with miR-138 mimic or hTERT shRNA plasmid and treatment with APG

SK-N-DZ and SK-N-BE2 cells were separately seeded at a concentration of  $5 \times 10^5$  cells per well in 6-well plates. On the next day, the cells were transfected with the miR-138 oligomeric RNA (50 nM) or a plasmid vector carrying hTERT shRNA (1 µg/ml) using Lipofectamine 2000 reagent (Invitrogen, Carlsbad, CA, USA) following the manufacturer's protocol. After 12 h of transfection, the old medium was replaced with fresh growth medium containing 2% FBS and 100 µM APG, and incubated for another 24 h. A dose of 100 µM APG was selected based on a dose-response study for cell viability, as determined by the 3-(4,5-dimethylthiazol-2-yl)-2,5-diphenyl tetrazolium bromide (MTT) assay (data not shown). The MTT assay showed that higher concentrations of APG did not significantly decrease cell viability, whereas lower concentrations were found to be less effective. A set of cultures was also transfected with the plasmid vector carrying the scrambled shRNA sequence for hTERT.

### RNA extraction and reverse transcription (RT) for miR-138

Total RNA was extracted from  $3 \times 10^6$  cells, which were transfected with hTERT shRNA (1 µg/ml) and treated with 100 µM APG, using TRIZOL (Invitrogen, Carlsbad, CA, USA) according to the manufacturer's protocol. Isolated total RNA was briefly exposed to RNase-free DNase I and 1 µg total RNA was reverse transcribed to cDNA using the gene-specific primers [21] and Thermoscript reverse transcriptase (Invitrogen, Carlsbad, CA, USA). The gene-specific miR-138 and U6 RNA antisense primers (10 µM stock) were used for the study.

### Use of polymerase chain reaction (PCR) for amplification of the RT product of miR-138

RT product of miR-138 or U6 RNA control was used as a template in a 25-µl PCR reaction. Briefly, PCR reaction was performed after

mixing 0.5 µl of miR-138 specific primers (10 µM), 2.5 µl of PCR buffer (10 µl), 0.75 µl of MgCl<sub>2</sub> (50 mM), 0.5 µl of dNTPs (10 mM, Invitrogen, Carlsbad, CA, USA), 0.2 µl of Taq Platinum DNA polymerase (5 U/µl, Invitrogen, Carlsbad, CA, USA) and 2 µl of RT product in a PCR thermal cycler (Eppendorf mastercycler gradient). The cycling protocol consisted of an initial 10 min denaturation step at 95 °C, followed by 35 cycles of PCR amplification of the transcripts using a program (denaturation at 95 °C for 15 s, and annealing at 52 °C for 30 s, and 72 °C extension for 30 s), and final extension at 72 °C for 7 min. The amplified RT-PCR products were resolved on 2.2% agarose gels by static-field electrophoresis, stained with ethidium bromide (1 µg/ml), destained the background of gels in water, visualized on a UV (303 nm) transilluminator, and photographed digitally using the UVDI Compact Digimage System (Major Science, Saratoga, CA, USA).

### Real-time quantitative RT-PCR (qRT-PCR) for miR-138

The expression of the miR-138 precursor was determined using real-time qRT-PCR following a recent report [22], with several modifications [23,24]. Master mix (3 µl) containing all of the reaction components except the primers were dispensed into a real-time qRT-PCR plate (Life Technologies, Grand Island, NY, USA). The master mix contained 0.5 µl of 10xPCR buffer, 0.7 µl of 25 mM MgCl<sub>2</sub>, 0.1 µl of 12.5 mM dNTPs, 0.01 µl of UNG, 0.025 µl of AmpliTaq Gold DNA polymerase, 0.5 µl of dilute cDNA (1:100) and water to 3 µl. All of the PCR reagents were from the SYBR green core reagent kit (Life Technologies, Grand Island, NY, USA). miR-138 and U6 RNA control were assayed in duplicates in the reaction plate. Real-time qRT-PCR was performed on an Applied Biosystems 7900HT real-time qRT-PCR instrument. PCR amplification was performed for 15 s at 95 °C and 1 min at 60 °C for 40 cycles followed by the thermal denaturation protocol. The expression of miR-138 relative to U6 RNA control was determined using the 2<sup>-ΔCT</sup> method [25]. To simplify the presentation of the data, the relative expression values were multiplied by 10<sup>2</sup>.

### Determination of cell viability using the MTT assay

The cell viability was determined by the MTT assay after transfection with scrambled miR-138 mimic, hTERT shRNA plasmid, miR-138 mimic, or/and APG treatment. Prior to transfection and treatment, the cells were seeded into 96-well microculture plates at 1 × 10<sup>4</sup> cells/well and allowed to attach overnight. Two control cultures were also used, one untreated control (CTL) and another transfected with the 50 nM scrambled miR-138 sequence for 12 h. After transfection or/and APG treatment and 36 h incubation, the old medium was discarded and a fresh medium containing MTT (0.2 mg/ml) was added and cells were incubated again for 3 h. Then, DMSO (200 µl) was added to each well to dissolve the formazan crystals and absorbance was measured at 570 nm wavelength using a multi-well plate reader (BioTek, Winooski, VT, USA). Cell viability was presented as percentage of viable cells in total population.

### Clonogenic assay for determination of cell survival and proliferation

Clonogenic assay or colony formation assay [26] was carried out using SK-N-DZ and SK-N-BE2 cells to study the effects of

transfection with miR-138 mimic or hTERT shRNA plasmid and APG treatment on colony formation. Both SK-N-DZ and SK-N-BE2 cells were transfected with miR-138 mimic or hTERT shRNA plasmid for 12 h, and treated with APG for 24 h. The cells were harvested using TrypLE Express (Invitrogen, Carlsbad, CA, USA) and 200 cells were seeded into 6-well plates. The cells were allowed to attach for 5 h and again transfected with miR-138 mimic or hTERT shRNA plasmid and treated with APG for 24 h. The cultures were terminated on day 10, fixed with 6% (v/v) glutaraldehyde, stained with 0.5% (w/v) crystal violet, and colonies were counted using a stereomicroscope. Small colonies formed from less than 50 cells were not scored for survival and proliferation.

### Annexin V-fluorescein isothiocyanate (FITC)/propidium iodide (PI) double staining and flow cytometry for analysis of the early phase of apoptosis

Cells were harvested after transfection or/and APG treatment as described above, and washed with phosphate-buffered saline (PBS, pH 7.4) twice before being fixed with 70% (vv) ethanol for 15 min. Subsequently, the cells were centrifuged to obtain pellets and residual ethanol was aspirated. Cells were then digested with DNase-free RNase A (2 mg/ml) for 30 min at 37 °C. Annexin V-FITC/PI double staining of the cells was performed as per manufacturer's instructions (BD Biosciences, San Jose, CA, USA), and then analyzed on an Epics XL-MCL Flow Cytometer (Beckman Coulter, Fullerton, CA, USA). Cells that were PI positive and Annexin V negative were considered as mechanically injured (quadrant A1), cells that were both PI and Annexin V positive (quadrant A2) were considered as late necrotic, both PI and Annexin V negative cells (quadrant A3) were considered as normal, and PI negative and Annexin V positive cells were considered as early apoptotic (quadrant A4). Flow cytometry detected the Annexin V positive cells with externalization of membrane phospholipids, an early biochemical feature of apoptosis. The Annexin V stained apoptotic cells were analyzed for statistical significance.

### In situ ApopTag assay to detect the late phase of apoptosis

Cells were grown on Lab-Tek chambered cover glasses (Nunc, Rochester, NY, USA). After transfection or/and APG treatment as described above, both adherent and non-adherent cells were allowed to settle on the cover glasses and then subjected to the in situ ApopTag assay. All cells were fixed in methanol before examination of induction of the nuclear DNA fragmentation or the late phase of apoptosis by the in situ ApopTag assay. ApopTag assay kit (Intergen, Purchase, NY, USA) was used for biochemical detection of nuclear DNA fragmentation that occurred at the late phase of apoptosis. The nuclei containing apoptotic DNA fragments were stained sharp brown with the in situ ApopTag assay and were not counterstained with methyl green that, however, stained the normal nuclei moderate to intense green. After the in situ ApopTag assay, cell were examined under the Olympus BX53 versatile system microscope (Olympus America, Center Valley, PA, USA) and photographed. The ApopTag positive cells were counted randomly in different fields to determine the percentage of apoptosis.

## Antibodies and Western blotting for molecules involved in apoptosis in cell cultures

Monoclonal primary IgG antibody against  $\beta$ -actin (clone AC-15) was purchased (Sigma-Aldrich, St. Louis, MO, USA) and used to monitor the equal loading of cytosolic proteins on sodium dodecyl sulfate-polyacrylamide gel electrophoresis (SDS-PAGE) experiments. Both SK-N-DZ and SK-N-BE2 cells were subjected to transfection with miR-138 mimic or hTERT shRNA plasmid followed by APG treatment, as described above, prior to extraction of protein samples. Protein samples obtained from cells were resolved on the SDS-PAGE gels, electroblotted to membranes, and probed with the primary IgG antibody against caspase-8, tBid, Bax, Bcl-2, Smac, survivin, calpain, caspase-3, spectrin break down product (SBDP), or inhibitor of caspase-activated DNase (ICAD). Primary IgG antibodies against all these proteins were procured from Santa Cruz Biotechnology (Santa Cruz, CA, USA). The horse-radish peroxidase conjugated goat anti-mouse or anti-rabbit secondary IgG antibody (Santa Cruz, CA, USA) was used to detect a primary IgG antibody. Western blots were incubated with enhanced chemiluminescence (ECL) detection reagents (GE Healthcare, Little Chalfont, Buckinghamshire, UK) and exposed to X-OMAT AR films (Eastman Kodak, Rochester, NY, USA) for autoradiography. The autoradiograms were scanned on an EPSON Scanner using Photoshop software (Adobe Systems, Seattle, WA, USA). All experiments were performed in triplicates.

## Development of subcutaneous neuroblastoma xenografts in nude mice and treatments

We conducted our animal studies in strict accordance with the recommendations in the 'Guide for the Care and Use of Laboratory Animals' of the National Institutes of Health and also with the approval from the Institutional Animal Care and Use Committee (IACUC) of the University of South Carolina (Columbia, SC, USA). We performed all surgical procedures under anesthesia condition and made all efforts to minimize animal suffering. For using the cells in development of xenografts, about 80% confluent cultures of SK-N-DZ and SK-N-BE2 cells were separately harvested, counted, and suspended in an equal volume of high-concentrated Matrigel (BD Biosciences, San Jose, California, USA). We used 100  $\mu$ l of cell suspension ( $5 \times 10^6$  cells) in Matrigel to inject subcutaneously in 6-week old nude mice (Charles River Laboratories, Wilmington, MA, USA). The animals were left for 1 week without any treatment for development of neuroblastoma xenografts. Treatments were carried out after 1 week when each tumor reached the size of around 10 mm in diameter. The animals were then divided into 4 groups of 6 mice in each group. One group of tumor bearing mice received no treatment and considered as untreated control (CTL). Other tumor bearing mice were injected at the tumor site carefully with miR-138 mimic (50  $\mu$ g DNA/injection/mouse), hTERT shRNA plasmid (50  $\mu$ g DNA/injection/mouse) and APG (10  $\mu$ g/injection/mouse), or miR-138 mimic (50  $\mu$ g DNA/injection/mouse) and APG (10  $\mu$ g/injection/mouse) on alternate days for 2 weeks. At the end of 3rd week, all animals were anesthetized with intraperitoneal injection of a mixture of ketamine (50 mg/kg) and xylazine (35 mg/kg) and photographed. Solid tumors were surgically removed, tumor weights were recorded, and tumors were photographed.

Tumors were surgically removed and used immediately for some experiments or stored at  $-80^\circ\text{C}$  for other experiments.

## Histopathological changes after miR-138 mimic or hTERT shRNA transfection and APG treatment

After completion of treatment schedule, mice were sacrificed and neuroblastoma xenografts were surgically collected as described above. After washing with PBS (pH 7.4), tumors were immediately frozen ( $-80^\circ\text{C}$ ) in Optima Cutting Temperature media (Fisher Scientific, Suwanee, GA, USA) and 10  $\mu$ m sections were cut with Microm HM 505 N (Labequip, Markham, Ontario, Canada). The sections were subjected to conventional hematoxylin and eosin (H&E) staining, examined under Olympus BX53 versatile system microscope (Olympus America, Center Valley, PA, USA), and photographed. The total population of apoptotic dead cells as observed on the H&E stained tumor sections were counted and analyzed for statistical significance.

## Western blotting for molecules involved in apoptosis in solid tumors

Western blotting was also carried out using the SK-N-DZ and SK-N-BE2 tumor samples for examination of specific molecules involved in apoptosis after the transfection and treatment. The solid tumors were weighed, cut into small pieces, and homogenized using an Omni Ruptor 400 Ultrasonic homogenizer (Omni International, Kennesaw, GA, USA). The homogenized tumor samples were centrifuged at 15,000g for 10 min at  $4^\circ\text{C}$  and the supernatants were collected. Protein concentration in the supernatant was determined using the Coomassie-Plus protein assay (Pierce Biotechnology, Rockford, IL, USA) and the samples were stored at  $-20^\circ\text{C}$  until used for Western blotting. Western blotting was performed, as described above, using these protein samples and the primary IgG antibodies against caspase-8, tBid, Bax, Bcl-2, Smac, survivin, calpain, caspase-3, and SBDP.

## Statistical analysis

The results from some of the experiments were analyzed for statistical significance using Minitab 16 statistical software (Minitab, State College, PA, USA). Data were expressed as mean  $\pm$  standard error of mean (SEM) of separate experiments ( $n \geq 3$ ) and compared by one-way analysis of variance (ANOVA) followed by the Fisher's post-hoc test. Difference between a control (CTL) group and a treatment group was considered significant at  $p < 0.05$ .

## Results

### Levels of miR-138 expression after hTERT shRNA transfection and APG treatment

To examine any alterations in miR-138 expression in human malignant neuroblastoma SK-N-DZ and SK-N-BE2 cells after hTERT shRNA transfection and APG treatment, we performed first semi-quantitative RT-PCR and then real-time qRT-PCR experiments (Fig. 1). As revealed from the resolved RT-PCR products on the 2.2% agarose gels, expression of the tumor suppressor miR-138 was clearly elevated after combination therapy in both cell lines (Fig. 1A).



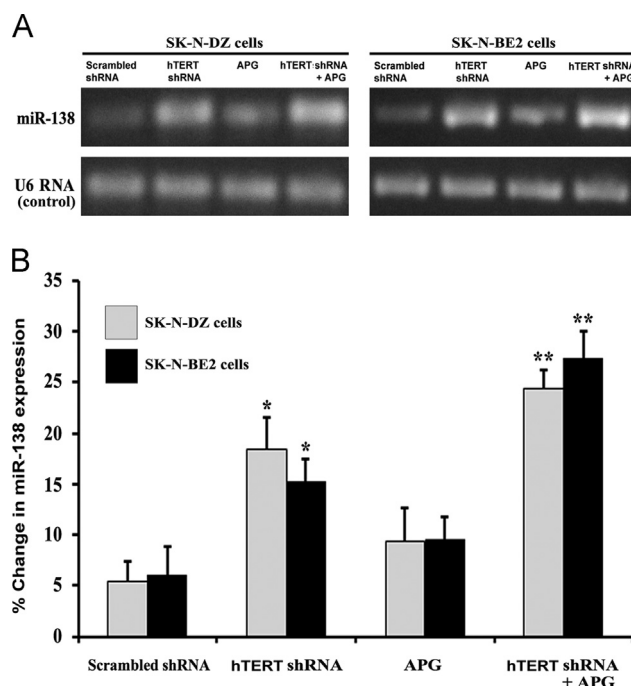


**Fig. 1 – Semi-quantitative RT-PCR and real-time qRT-PCR for levels of expression of pre-miR-138 in human malignant neuroblastoma SK-N-DZ and SK-N-BE2 cells.** Treatments: transfection with plasmid vector carrying scrambled shRNA (1  $\mu$ g/ml) for 12 h, transfection with plasmid vector carrying hTERT shRNA (1  $\mu$ g/ml) for 12 h, 100  $\mu$ M APG for 24 h, and hTERT shRNA (1  $\mu$ g/ml) for 12 h+100  $\mu$ M APG for 24 h. (A) Semi-quantitative RT-PCR for levels of expression of miR-138. Expression of U6 RNA was used as a loading control. The RT-PCR products were resolved on 2.2% agarose gels by electrophoresis. (B) Real-time qRT-PCR for relative levels of expression of miR-138 after normalizing with U6 RNA (control). Difference between scrambled shRNA and a monotherapy or combination therapy was considered significant at \* $p < 0.05$  or \*\* $p < 0.01$ .

Further, real-time qRT-PCR analyses were performed to quantify the levels of miR-138 expression in both cell lines after transfection and treatment (Fig. 1B). We did not observe any difference in miR-138 expression between scrambled hTERT shRNA plasmid transfected cells and untreated control cells (data not shown). Therefore, scrambled hTERT shRNA plasmid was used as the control vector in the experiments. Transfection of cells with hTERT shRNA alone was more effective than treatment of cells with APG alone in increasing miR-138 expression. Interestingly, when compared with a monotherapy (scrambled shRNA, hTERT shRNA, or APG), combination of hTERT shRNA and APG most significantly increased the levels of miR-138 expression in both cell lines. Combination therapy was so effective that it could cause almost 5 times higher miR-138 expression than scrambled shRNA in both cell lines.

#### More power of miR-138 mimic than hTERT shRNA plasmid in potentiating efficacy of APG in decreasing both cell viability and colony formation

We determined cell viability and colony forming ability of the cells after transfection with miR-138 mimic or hTERT shRNA

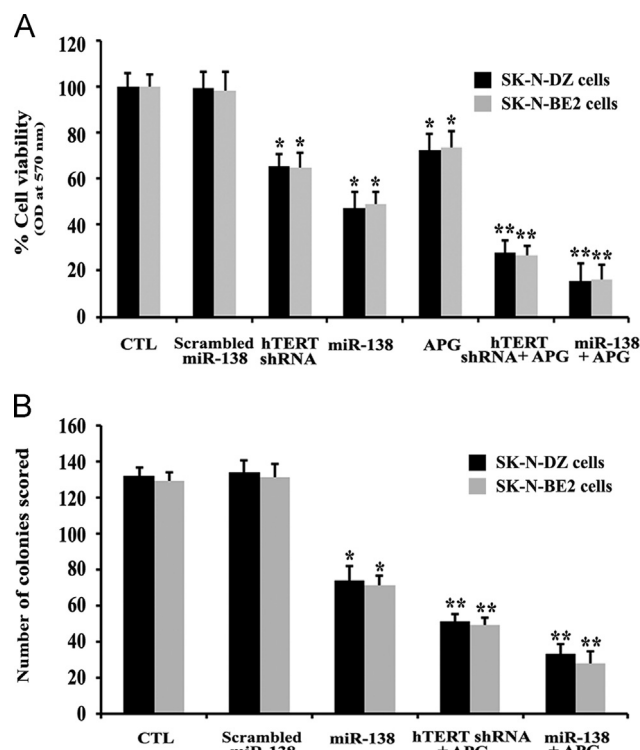


**Fig. 2 – Determination of residual cell viability and colony forming ability of SK-N-DZ and SK-N-BE2 cells after treatments.** (A) MTT assay for determination of residual cell viability. Treatments: control (CTL), scrambled miR-138 mimic (50 nM) for 12 h, hTERT shRNA plasmid (1  $\mu$ g/ml) for 12 h, miR-138 mimic (50 nM) for 12 h, 100  $\mu$ M APG for 24 h, hTERT shRNA plasmid (1  $\mu$ g/ml) for 12 h+100  $\mu$ M APG for 24 h, and miR-138 mimic (50 nM) for 12 h+100  $\mu$ M APG for 24 h. (B) Clonogenic assay for evaluation of cell survival and proliferation. Treatments: CTL, scrambled miR-138 mimic (50 nM) for 12 h, miR-138 mimic (50 nM) for 12 h, hTERT shRNA plasmid (1  $\mu$ g/ml) for 12 h+100  $\mu$ M APG for 24 h, and miR-138 mimic (50 nM) for 12 h+100  $\mu$ M APG for 24 h. Then, cells were harvested, 200 cells were seeded in 6-well plates, allowed to attach for 5 h, and again treated similarly with scrambled miR-138 mimic, miR-138 mimic, hTERT shRNA plasmid, and APG as described above. Difference between CTL or scrambled miR-138 and a monotherapy or a combination therapy was considered significant at \* $p < 0.05$  or \*\* $p < 0.01$ .

plasmid and treatment with APG alone and in combination in both SK-N-DZ and SK-N-BE2 cell lines (Fig. 2). We observed significant decreases in cell viability after miR-138 overexpression, hTERT knockdown, or APG treatment (Fig. 2A). Untreated control (CTL) and scrambled miR-138 transfection equally maintained cell viability in both neuroblastoma cell lines. Interestingly, miR-138 overexpression was more effective than hTERT knockdown or APG treatment alone in decreasing cell viability in both cell lines. Among all the strategies (Fig. 2A), miR-138, hTERT shRNA and APG, and miR-138 and APG were effective in causing around 54%, 75%, and 85% cell death, respectively, in both cell lines. So, we decided to explore comparative efficacies of these three strategies in our clonogenic assay (Fig. 2B) and all subsequent experiments. Clonogenic assay is based on the ability

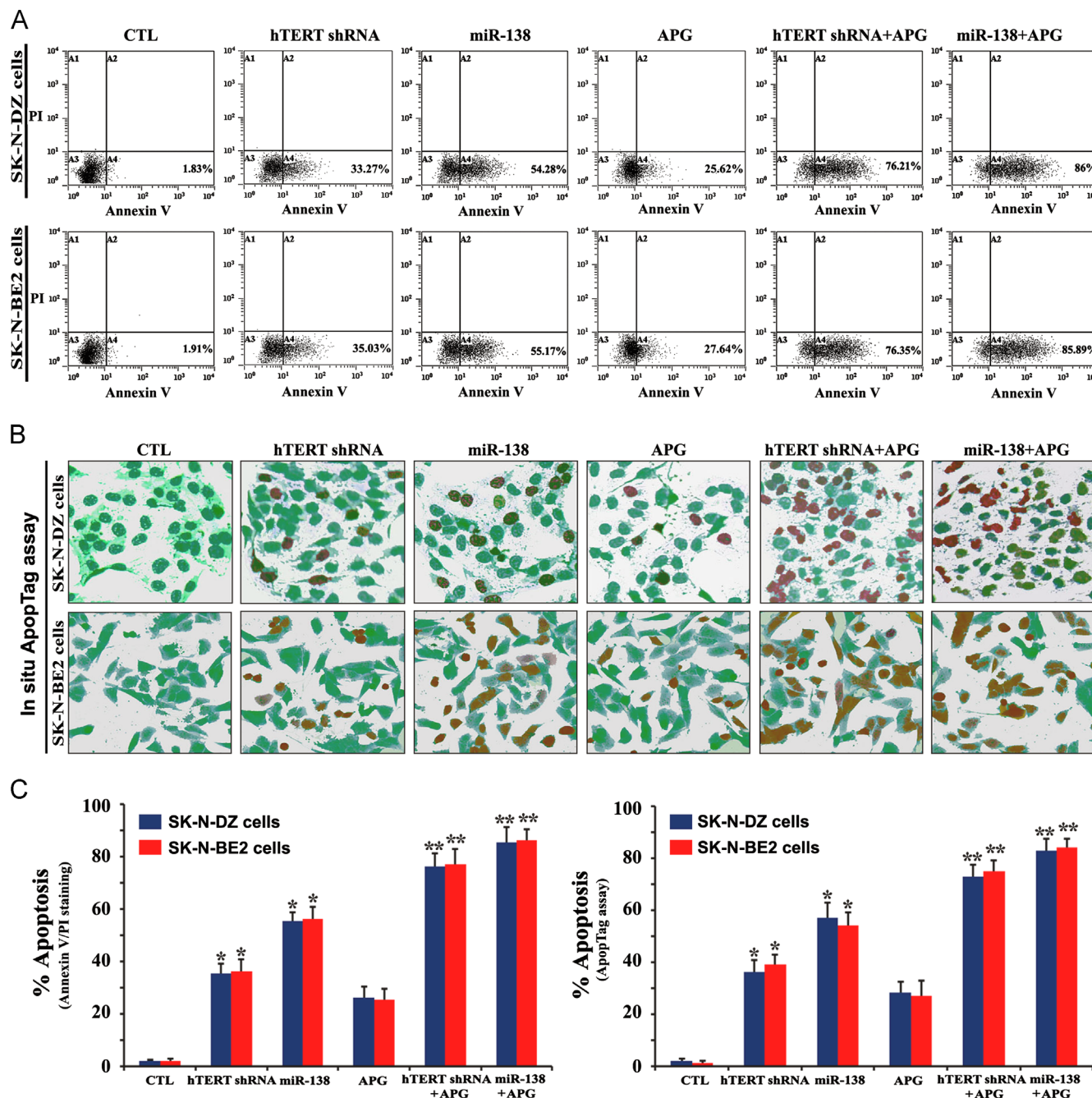


**Fig. 3 – Flow cytometry and in situ ApopTag assay for detection and determination of amounts of apoptosis in SK-N-DZ and SK-N-BE2 cells. Treatments:** control (CTL), hTERT shRNA plasmid (1  $\mu$ g/ml) for 12 h, miR-138 mimic (50 nM) for 12 h, 100  $\mu$ M APG for 24 h, hTERT shRNA plasmid (1  $\mu$ g/ml) for 12 h+100  $\mu$ M APG for 24 h, and miR-138 mimic (50 nM) for 12 h+100  $\mu$ M APG for 24 h. (A) Annexin V-FITC/PI double staining followed by flow cytometry to detect the early phase of apoptosis. (B) In situ ApopTag assay to detect the late phase of apoptosis. (C) The percentages of apoptotic cells are shown in bar diagrams based on results from three independent experiments. Difference between untreated CTL and a treatment group was considered significant at \* $p$ <0.05 or \*\* $p$ <0.01.

of a single cell to form a multicellular colony of a minimum of 50 cells within a particular time frame. When compared with miR-138 alone or combination of hTERT shRNA and APG, we found that combination miR-138 and APG most significantly decreased the colony forming ability of the cells (Fig. 2B). These results clearly indicated that direct miR-138 overexpression was more powerful than hTERT knockdown in potentiating the efficacy of APG treatment in decreasing cell viability as well as

colony formation ability of human malignant neuroblastoma cells.

#### Flow cytometry and in situ ApopTag assay showed amounts of apoptosis in SK-N-DZ and SK-N-BE2 cells

The effects of transfection with miR-138 mimic or hTERT shRNA plasmid and treatment with APG alone and in combination for

induction of the early phase of apoptosis and also the late phase of apoptosis were investigated by flow cytometry and in situ ApopTag assay, respectively (Fig. 3). Flow cytometric diagrams (Fig. 3A) demonstrated that cells with mechanical injury (quadrant A1) or narcosis (quadrant A2) were less than 1% of total population in any treatment group and all cells were found in only one spot (quadrant A3) after no treatment but cells were partly prone to only apoptotic death (quadrant A4) after a monotherapy or combination therapy (Fig. 3A). Further, in situ ApopTag assay was used to examine the nuclear DNA fragmentation or the late phase of apoptosis in the cells after transfection and treatment (Fig. 3B). Both control cell lines showed negligible or no brown staining, indicating almost absence of ApopTag positive cells or late phase of apoptosis. On the other hand, cells subjected to hTERT shRNA and APG, or miR-138 and APG indicated massive brown staining due to induction of the late phase of apoptosis in the cells. We determined the amounts of apoptotic cells following flow cytometry and in situ ApopTag assay (Fig. 3C). Transfection with miR-138 mimic or hTERT shRNA and also treatment with APG alone caused significant apoptotic death in both cell lines (Fig. 3C). Combination of hTERT shRNA and APG caused about 76% apoptosis while combination of miR-138 mimic and APG induced almost 86% apoptosis in both cell lines (Fig. 3C), indicating that miR-138 mimic was more powerful than hTERT shRNA in potentiating APG for induction of apoptotic death in human malignant neuroblastoma cells.

### Molecular mechanisms of induction of apoptosis in malignant neuroblastoma cells after transfection with miR-138 mimic or hTERT shRNA plasmid and treatment with APG

To determine the plausible molecular mechanisms of induction of apoptosis in human malignant neuroblastoma cells after miR-138 mimic or hTERT shRNA plasmid transfection and APG treatment, we performed Western blotting using some primary antibodies against key molecules involved in regulation of apoptotic death (Fig. 4). Our results showed activation of extrinsic pathway of apoptosis with increase in active caspase-8 for proteolytic generation of tBid in both SK-N-DZ and SK-N-BE2 cells following monotherapy and combination therapy. Activation of intrinsic pathway of apoptosis also occurred as evidenced from an increase in expression of Bax (pro-apoptotic protein) and decrease in expression of Bcl-2 (anti-apoptotic protein), resulting in an increase in Bax:Bcl-2 ratio in both cell lines. Evidently, combination of miR-138 overexpression and APG treatment was more effective than combination of hTERT knockdown and APG treatment in causing more molecular alterations for induction of apoptosis via both extrinsic and intrinsic pathways. An increase in Bax:Bcl-2 ratio is known to alter mitochondrial permeability to release Smac into the cytosol, promoting activation of intrinsic apoptotic cascade. Smac neutralizes a set of endogenous inhibitor-of-apoptosis proteins such as survivin so as to facilitate activation of caspase-3. We found activation of both calpain and caspase-3

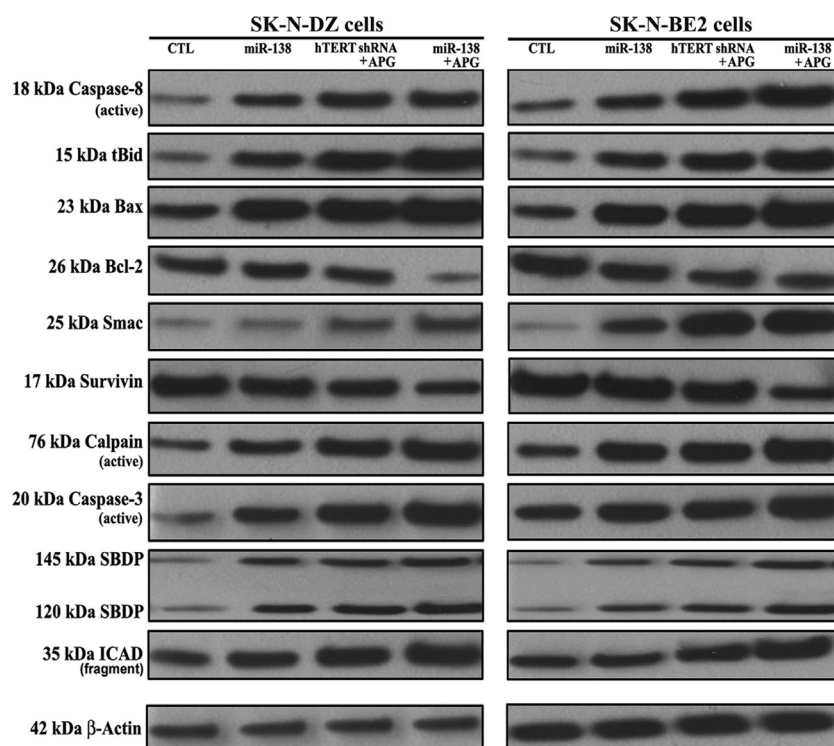


**Fig. 4 – Western blotting for examination of the molecules of the extrinsic and intrinsic pathways of apoptosis in SK-N-DZ and SK-N-BE2 cells. Treatments: control (CTL), miR-138 mimic (50 nM) for 12 h, hTERT shRNA plasmid (1 µg/ml) for 12 h+100 µM APG for 24 h, and miR-138 mimic (50 nM) for 12 h+100 µM APG for 24 h. Representative Western blots ( $n \geq 3$ ) to show expression and activation of selective molecules involved in the induction of extrinsic and intrinsic pathways of apoptosis. Expression of  $\beta$ -actin was used as a loading control.**



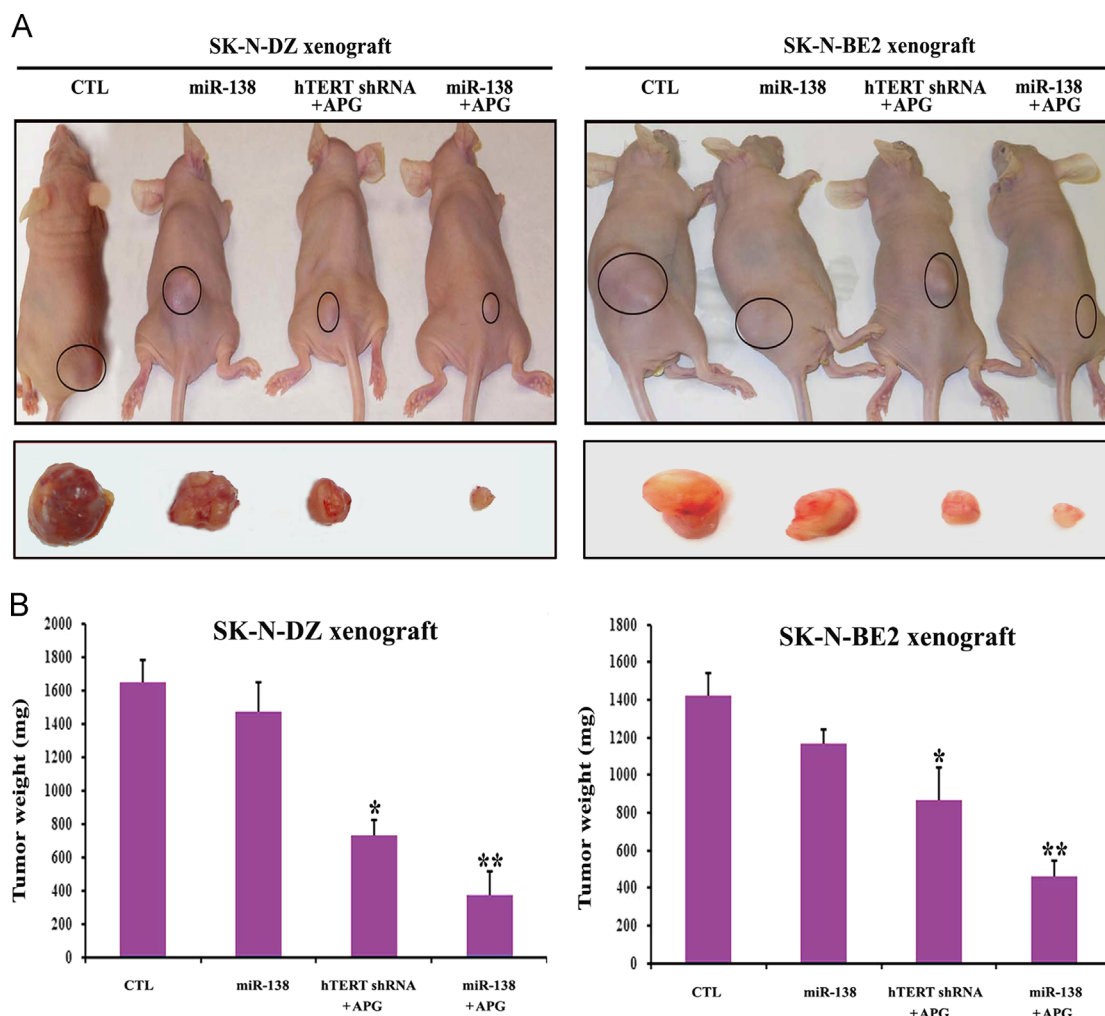


**Fig. 5 – Regression of SK-N-DZ and SK-N-BE2 tumors in nude mice after the treatments.** Treatments: control (CTL, no treatment for 21 days), tumor bearing mice (7 days after tumor implantation) were injected at the tumor site with miR-138 mimic (50  $\mu$ g RNA/injection/mouse), hTERT shRNA plasmid (50  $\mu$ g DNA/injection/mouse)+APG (10  $\mu$ g/injection/mouse), and miR-138 mimic (50  $\mu$ g RNA/injection/mouse)+APG (10  $\mu$ g/injection/mouse) on alternate days for 2 weeks. All animals were then sacrificed for analyzing the tumors. (A) Mice with SK-N-DZ and SK-N-BE2 xenografts. (B) Bar graphs for presenting regression of tumors. We used 6 animals per group. Difference between CTL group and a treatment group was considered significant at \* $p < 0.05$  or \*\* $p < 0.01$ .

that caused proteolysis of  $\alpha$ -spectrin to generate calpain-specific 145 kDa SBDP and caspase-3-specific 120 kDa SBDP, respectively, in course of apoptosis in both cell lines. Activate caspase-3 also caused cleavage and inactivation of the inhibitor of caspase-activated DNase (ICAD) to release caspase-activated DNase (CAD) for translocation to the nucleus for fragmentation of nuclear DNA. Combination of miR-138 mimic and APG treatment was the most effective strategy for activation of caspase-3 and cleavage of ICAD in both cell lines. Almost uniform expression of  $\beta$ -actin in all treatments served as an internal control and indicated equal amounts of protein loadings in all lanes.

#### Combination of miR-138 mimic transfection and APG treatment most effectively decreased tumor growth and induced apoptosis in malignant neuroblastoma xenografts

Our in vivo studies showed the comparative effectiveness of miR-138 overexpression, hTERT knockdown, and APG

treatment in reducing the tumor growth and inducing apoptotic death in both SK-N-DZ and SK-N-BE2 xenografts in nude mice (Figs. 5 and 6). Compared with untreated control (CTL), miR-138 overexpression alone reduced tumor growth (Fig. 5A) but not significantly (Fig. 5B). Importantly, combination of miR-138 overexpression and APG treatment showed the highest efficacy in reducing tumor growth (Fig. 5A) and more significant efficacy than combination of hTERT knockdown and APG treatment in decreasing tumor weight (Fig. 5B). Following the treatments, we performed H&E staining of the tumor sections for examination of induction of cell death (Fig. 6). We found that CTL groups maintained characteristic tumor growth, miR-138 overexpression alone induced apoptotic death to some extent, but combination of miR-138 overexpression and APG treatment induced apoptotic death most extensively in both malignant neuroblastoma xenograft models (Fig. 6A). Quantitative analyses of apoptotic tumor cells revealed the extents of induction apoptosis following treatments with miR-138 alone (about 160 cells/field), combination



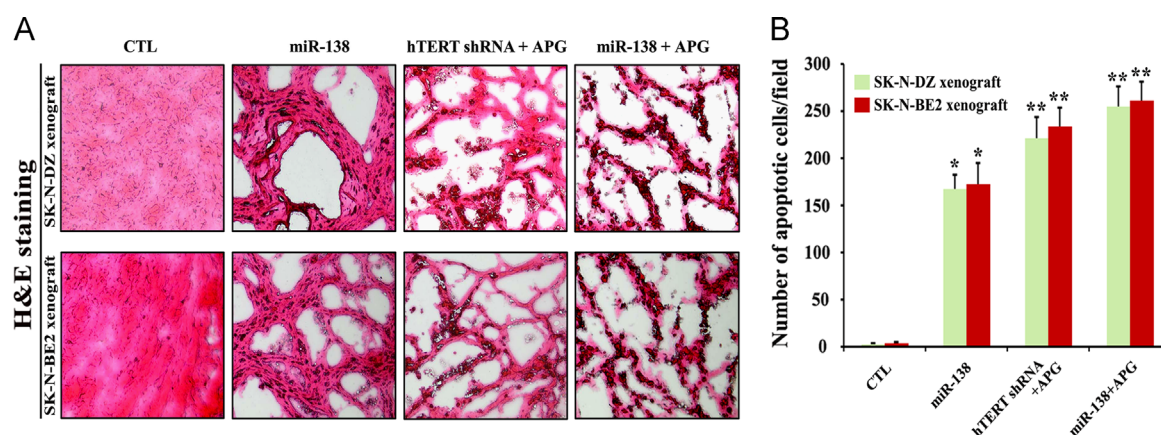


**Fig. 6 – Evaluation of histopathological changes in the SK-N-DZ and SK-N-BE2 tumors after treatments.** Treatments: control (CTL, no treatment for 21 days), tumor bearing mice (7 days after tumor implantation) were injected at the tumor site with miR-138 mimic (50  $\mu$ g RNA/injection/mouse), hTERT shRNA plasmid (50  $\mu$ g DNA/injection/mouse)+APG (10  $\mu$ g/injection/mouse), and miR-138 mimic (50  $\mu$ g RNA/injection/mouse)+APG (10  $\mu$ g/injection/mouse) on alternate days for 2 weeks. All animals were then sacrificed for analyzing the histopathological changes in the tumors. (A) H&E staining to examine histopathological changes in the xenograft sections. (B) The apoptotic cells in SK-N-DZ and SK-N-BE2 xenografts were shown in bar diagrams based on observation from three independent microscopic fields. Difference between CTL group and a treatment group was considered significant at \* $p < 0.05$  or \*\* $p < 0.01$ .

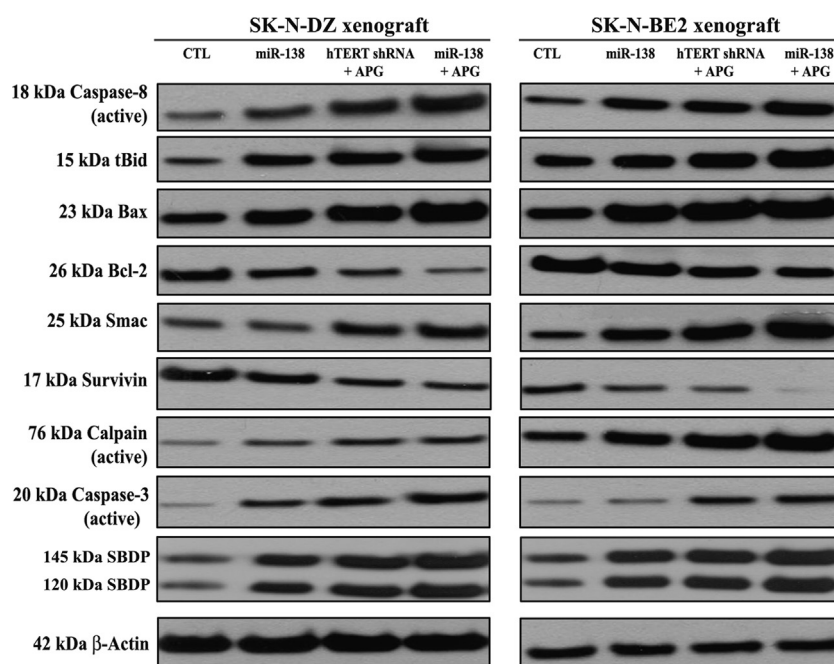


**Fig. 7 – Changes in expression of apoptotic proteins in SK-N-DZ and SK-N-BE2 tumors after treatments.** Treatments: control (CTL, no treatment for 21 days), tumor bearing mice (7 days after tumor implantation) were injected at the tumor site with miR-138 mimic (50  $\mu$ g RNA/injection/mouse), hTERT shRNA plasmid (50  $\mu$ g RNA/injection/mouse)+APG (10  $\mu$ g/injection/mouse), and miR-138 mimic (50  $\mu$ g RNA/injection/mouse)+APG (10  $\mu$ g/injection/mouse) on alternate days for 2 weeks. All animals were then sacrificed for analyzing the molecular changes in the tumors. Representative Western blots ( $n \geq 3$ ) to show expression and activation of selective molecules involved in the induction of extrinsic and intrinsic pathways of apoptosis. Expression of  $\beta$ -actin was used as a loading control.

of hTERT shRNA and APG (about 220 cells/field), and combination of miR-138 and APG (about 260 cells/field) in both SK-N-DZ and SK-N-BE2 xenograft models (Fig. 6B). Therefore, miR-138 mimic was more effective than hTERT shRNA plasmid in enhancing efficacy of APG for inducing the most significant amounts of apoptosis in human malignant neuroblastomas in vivo.

#### Combination of miR-138 mimic transfection and APG treatment most effectively modulated the molecular events of extrinsic and intrinsic pathways for apoptosis in neuroblastoma xenografts

We performed Western blotting to investigate the effects of miR-138 mimic, hTERT shRNA and APG, and miR-138 mimic and APG

on the molecular events of apoptosis in human malignant neuroblastomas in vivo (Fig. 7). Western blotting revealed that these therapeutic strategies progressively generated active caspase-8 that proteolytically produced tBid for its translocation to mitochondria, indicating activation of molecular components of the extrinsic pathway of apoptosis to augment the intrinsic pathway of apoptosis. But maximum activation of caspase-8 and also production of tBid occurred after treatment with combination of miR-138 mimic and APG in both neuroblastoma xenograft models. Also, miR-138 overexpression followed by APG treatment dramatically increased Bax expression and decreased in Bcl-2 expression, resulting in the Bax:Bcl-2 ratio to directly trigger intrinsic pathway of apoptosis with mitochondrial release of Smac into the cytosol for down regulation and degradation of survivin and activation of caspase-3. The active subunits of calpain and caspase-3 were most prominently increased for proteolytic generation of calpain-specific 145 kDa SBDP and caspase-3-specific 120 kDa SBDP, respectively, in both neuroblastoma xenograft models after treatment with combination of miR-138 mimic and APG. Reprobing of the Western blots demonstrated almost uniform expression of  $\beta$ -actin and thus equal loading of proteins in all lanes.

## Discussion

Our present study demonstrates that direct miR-138 overexpression followed by APG treatment is more powerful than hTERT knockdown followed by APG treatment in inhibiting cell proliferation and induction of apoptosis in human malignant neuroblastoma SK-N-DZ and SK-N-BE2 cells both in vitro and in vivo. Studies of molecular events showed that combination of miR-138 mimic and APG was more effective than combination of hTERT shRNA and APG in altering the expression of the molecules for induction of extrinsic and intrinsic pathways of apoptosis in SK-N-DZ and SK-N-BE2 in cell culture and animal models. Thus, our current investigation indicates that direct miR-138 overexpression is more powerful than hTERT knockdown to potentiate APG for induction of apoptosis in human malignant neuroblastomas.

Our semi-quantitative RT-PCR and real-time qRT-PCR experiments showed clear increases in expression of the tumor suppressor miR-138 in both malignant neuroblastoma SK-N-DZ and SK-N-BE2 cells after treatment with combination of hTERT shRNA and APG (Fig. 1). So, hTERT knockdown and APG treatment could upregulate expression of miR-138, which might be involved in inhibition of cell proliferation and induction of apoptosis in human malignant neuroblastoma cells. After direct miR-138 overexpression and APG treatment, we observed the highest amounts of cell death and reductions in colony formation ability in human malignant neuroblastoma cells (Fig. 2). Our results from the Annexin V-FITC/PI double staining and the in situ ApopTag assay also showed the highest efficacy of miR-138 overexpression in potentiating APG for induction of apoptosis (Fig. 3) with the modulation of the molecular events related to this process (Fig. 4) in human malignant neuroblastoma cells. We also observed and validated similar results in our in vivo studies where growth and weight of the SK-N-DZ and SK-N-BE2 tumors were drastically inhibited following combination of miR-138 overexpression and APG treatment (Fig. 5). As evidenced from our H&E staining results, the most effective inhibition of the tumor growth was due

to apoptotic cell death, which was induced by combination of miR-138 overexpression and APG treatment (Fig. 6). Our Western blotting results clearly showed that miR-138 mimic could be a better choice than hTERT shRNA plasmid to use in combination with APG treatment for modulating the molecular events for the highest induction of extrinsic and intrinsic pathways of apoptosis in human malignant neuroblastoma cells both in vitro (Fig. 4) and in vivo (Fig. 7).

Caspase-8 mediated cleavage of Bid to tBid and the translocation of tBid to mitochondria provides a link between extrinsic and intrinsic pathways of apoptosis [27]. Caspase-8 mediated cleavage of Bid to tBid may also be associated with the alterations in expression of pro-apoptotic Bax protein and anti-apoptotic Bcl-2 protein [28]. Increase in Bax:Bcl-2 ratio is a key factor to induce the release of several pro-apoptotic molecules from mitochondria [29]. Upregulation of various anti-apoptotic molecules such as Bcl-2 protects the cancer cells from induction of apoptosis [30]. In the current study, we found that miR-138 mimic transfection followed by APG treatment could cause maximum upregulation of Bax with a concomitant down regulation of Bcl-2 so as to cause an increase in the Bax:Bcl-2 ratio in SK-N-DZ and SK-N-BE2 cells both in vitro and in vivo. Mitochondrial activation of the effector caspases, including caspase-3, can cleave a number of cytoplasmic and nuclear substrates leading to induction of apoptosis [29,31]. Simultaneous activation of both calpain and caspase-3 can play significant roles in induction of apoptosis in many human cancer cells. In the present study, we demonstrated that direct miR-138 overexpression in combination with APG treatment played an important role in dramatic increases in activation of calpain and caspase-3. Increases in the activities of calpain and caspase-3 were confirmed in the formation of 145 kDa SBDP and 120 kDa SBDP, respectively, in SK-N-DZ and SK-N-BE2 cells both in vitro and in vivo. Also, caspase-3 activity caused ICAD cleavage in both SK-N-DZ and SK-N-BE2 cells. Cleavage of ICAD could allow the human malignant neuroblastoma cells to translocate CAD to the nucleus for nuclear DNA fragmentation, the final step in apoptosis.

In conclusion, we have demonstrated that miR-138 acts as a potent tumor suppressor in human malignant neuroblastoma cells and its direct overexpression can potentiate the efficacy of APG for induction of molecular mechanisms of extrinsic and intrinsic pathways of apoptosis in different malignant neuroblastomas both in vitro and in vivo. Demonstration of direct miR-138 overexpression and APG treatment as an effective combination therapy for efficient treatment of human malignant neuroblastoma in cell culture and animal models is a highly significant finding. The use of direct miR-138 overexpression and APG treatment in combination for controlling growth human malignant neuroblastomas may provide a powerful therapeutic strategy, which may circumvent current issues of drug resistance and adverse side effects. Our current study suggests that more molecular mechanisms of therapeutic efficacy of the direct miR-138 overexpression and APG treatment should be explored to determine and establish the potential of this combination therapeutic strategy for successful treatment of malignant neuroblastoma in humans in the future.

## Conflict of interest disclosures

The authors have declared that no conflict of interest exists.

## Acknowledgments

This work was supported in part by a grant (R01 NS65456) from the National Institutes of Health (Bethesda, MD, USA) and another grant (SCIRF-11-002) from the South Carolina Spinal Cord Injury Research Foundation (Columbia, SC, USA).

## REFERENCES

- [1] M.M. Grinsell, V.F. Norwood. At the bottom of the differential diagnosis list: unusual causes of pediatric hypertension, *Pediatr. Nephrol.* 24 (2009) 2137–2146.
- [2] P. Trang, J.B. Weidhaas, F.J. Slack. MicroRNAs as potential cancer therapeutics, *Oncogene* 27 (2008) S52–S57.
- [3] S.K. Shenouda, S.K. Alahari. MicroRNA function in cancer: oncogene or a tumor suppressor?, *Cancer Metastasis Rev.* 28 (2009) 369–378.
- [4] S. Mitomo, C. Maesawa, S. Ogasawara, T. Iwaya, M. Shibazaki, A. Yashima-Abo, K. Kotani, H. Oikawa, E. Sakurai, N. Izutsu, K. Kato, H. Komatsu, K. Ikeda, G. Wakabayashi, T. Masuda. Down regulation of miR-138 is associated with overexpression of human telomerase reverse transcriptase protein in human anaplastic thyroid carcinoma cell lines, *Cancer Sci.* 99 (2008) 280–286.
- [5] M. Seike, A. Goto, T. Okano, E.D. Bowman, A.J. Schetter, I. Horikawa, E.A. Mathe, J. Jen, P. Yang, H. Sugimura, A. Gemma, S. Kudoh, C.M. Croce, C.C. Harris. miR-21 is an EGFR-regulated anti-apoptotic factor in lung cancer in never-smokers, *Proc. Nat. Acad. Sci. U.S.A.* 106 (2009) 12085–12090.
- [6] X. Zhao, L. Yang, J. Hu, J. Ruan. miR-138 might reverse multidrug resistance of leukemia cells, *Leukocyte. Res.* 34 (2010) 1078–1082.
- [7] X. Liu, C. Wang, Z. Chen, Y. Jin, Y. Wang, A. Kolokythas, Y. Dai, X. Zhou. MicroRNA-138 suppresses epithelial-mesenchymal transition in squamous cell carcinoma cell lines, *Biochem. J.* 440 (2011) 23–31.
- [8] K. Nakano, E. Watney, J.K. McDougall. Telomerase activity and expression of telomerase RNA component and telomerase catalytic subunit gene in cervical cancer, *Am. J. Pathol.* 153 (1998) 857–864.
- [9] T. Kanaya, S. Kyo, M. Takakura, H. Ito, M. Namiki, M. Inoue. hTERT is a critical determinant of telomerase activity in renal-cell carcinoma, *Int. J. Cancer* 78 (1998) 539–543.
- [10] S.S. Kang, T. Kwon, D.Y. Kwon, S.I. Do. Akt protein kinase enhances human telomerase activity through phosphorylation of telomerase reverse transcriptase subunit, *J. Biol. Chem.* 274 (1999) 13085–13090.
- [11] T.W. Park, S. Riethdorf, L. Riethdorf, T. Löning, F. Jänicke. Differential telomerase activity, expression of the telomerase catalytic sub-unit and telomerase-RNA in ovarian tumors, *Int. J. Cancer* 84 (1999) 426–431.
- [12] Y.W. Kim, S.Y. Hur, T.E. Kim, J.M. Lee, S.E. Namkoong, I.K. Ki, J.W. Kim. Protein kinase C modulates telomerase activity in human cervical cancer cells, *Exp. Mol. Med.* 33 (2001) 156–163.
- [13] L. Boldrini, P. Faviana, S. Gisfredi, Y. Zucconi, D. Di Quirico, V. Donati, P. Berti, R. Spisni, D. Galleri, G. Materazzi, F. Basolo, P. Miccoli, R. Pingitore, G. Fontanini. Evaluation of telomerase mRNA (hTERT) in colon cancer, *Int. J. Oncol.* 21 (2002) 493–497.
- [14] A.L. Ducrest, H. Szutorisz, J. Lingner, M. Nabholz. Regulation of the human telomerase reverse transcriptase gene, *Oncogene* 21 (2002) 541–552.
- [15] A.G. Bader, D. Brown, M. Winkler. The promise of microRNA replacement therapy, *Cancer Res.* 70 (2010) 7027–7030.
- [16] F. Petrocca, J. Lieberman. Micromanipulating cancer: microRNA-based therapeutics?, *RNA Biol.* 6 (2009) 335–340.
- [17] J. George, M. Tsutsumi. siRNA-mediated knockdown of connective tissue growth factor prevents N-nitrosodimethylamine-induced hepatic fibrosis in rats, *Gene Ther.* 14 (2007) 790–803.
- [18] J. George, N.L. Banik, S.K. Ray. Combination of hTERT knockdown and IFN-gamma treatment inhibited angiogenesis and tumor progression in glioblastoma, *Clin. Cancer Res.* 15 (2009) 7186–7195.
- [19] J. George, N.L. Banik, S.K. Ray. Combination of taxol and Bcl-2 siRNA induces apoptosis in human glioblastoma cells and inhibits invasion, angiogenesis and tumor growth, *J. Cell Mol. Med.* 13 (2009) 4205–4218.
- [20] S. Karmakar, K.A. Davis, S.R. Choudhury, A. Deeconda, N.L. Banik, S.K. Ray. Bcl-2 inhibitor and apigenin worked synergistically in human malignant neuroblastoma cell lines and increased apoptosis with activation of extrinsic and intrinsic pathways, *Biochem. Biophys. Res. Commun.* 388 (2009) 705–710.
- [21] S. Griffiths-Jones. The microRNA Registry, *Nucleic Acids Res.* 32 (2004) D109–D111.
- [22] J. Jiang, E.J. Lee, Y. Gusev, T.D. Schmittgen. Real-time expression profiling of microRNA precursors in human cancer cell lines, *Nucleic Acids Res.* 33 (2005) 5394–5403.
- [23] M. Chakrabarti, W. Ai, N.L. Banik, S.K. Ray. Overexpression of miR-7-1 increases efficacy of green tea polyphenols for induction of apoptosis in human malignant neuroblastoma SH-SY5Y and SK-N-DZ cells, *Neurochem. Res.* 38 (2013) 420–432.
- [24] M. Chakrabarti, M. Khandkar, N.L. Banik, S.K. Ray. Alterations in expression of specific microRNAs by combination of 4-HPR and EGCG inhibited growth of human malignant neuroblastoma cells, *Brain Res.* 1454 (2012) 1–13.
- [25] K.J. Livak, T.D. Schmittgen. Analysis of relative gene expression data using real-time quantitative PCR and the 2<sup>-</sup>(Delta Delta C (T)) method, *Methods* 25 (2001) 402–408.
- [26] N.A. Franken, H.M. Rodermond, J. Stap, J. Haveman, C. van Bree. Clonogenic assay of cells in vitro, *Nat. Protoc.* 1 (2006) 2315–2319.
- [27] S. Fulda, K.M. Debatin. Extrinsic versus intrinsic apoptosis pathways in anticancer chemotherapy, *Oncogene* 25 (2006) 4798–4811.
- [28] S.R. Choudhury, S. Karmakar, N.L. Banik, S.K. Ray. Valproic acid induced differentiation and potentiated efficacy of taxol and nanotaxol for controlling growth of human glioblastoma LN18 and T98G cells, *Neurochem. Res.* 26 (2011) 2292–2305.
- [29] S. Karmakar, N.L. Banik, S.J. Patel, S.K. Ray. Curcumin activated both receptor-mediated and mitochondria-mediated proteolytic pathways for apoptosis in human glioblastoma T98G cells, *Neurosci. Lett.* 407 (2006) 53–58.
- [30] J. George, N.L. Banik, S.K. Ray. Bcl-2 siRNA augments taxol mediated apoptotic death in human glioblastoma U138MG and U251MG cells, *Neurochem. Res.* 34 (2009) 66–78.
- [31] M.M. Hossain, N.L. Banik, S.K. Ray. Survivin knockdown increased anti-cancer effects of (–)-epigallocatechin-3-gallate in human malignant neuroblastoma SK-N-BE2 and SH-SY5Y cells, *Exp. Cell. Res.* 318 (2012) 1597–1610.